

Article

# Halloysite Nanotubes as Bimodal Lewis/Brønsted Acid Heterogeneous Catalysts for the Synthesis of Heterocyclic Compounds

Jiaying Yu <sup>1,2</sup>, Javier Mateos <sup>1</sup>  and Mauro Carraro <sup>1,3,\*</sup> <sup>1</sup> Department of Chemical Sciences, University of Padova, Via F. Marzolo 1, 35131 Padova, Italy<sup>2</sup> College of Chemistry and Environmental Engineering, Shenzhen University, 3688 Nanhai Ave, Shenzhen 518060, China<sup>3</sup> ITM-CNR, UoS of Padova, Via F. Marzolo 1, 35131 Padova, Italy

\* Correspondence: mauro.carraro@unipd.it

**Abstract:** Halloysite nanotubes can be used for the preparation of solid catalysts. Owing to their natural availability at low-cost as well as to their large and easy-to-functionalize surface, they can be conveniently activated with mineral acids or derivatized with acidic groups. Nevertheless, the use of HNTs as catalysts in complex transformations is still limited. Herein, we report two strategies to utilize HNT-based materials as solid acidic catalysts for the Biginelli reaction. To this aim, two methods for increasing the number of acidic sites on the HNTs were explored: (i) the treatment with piranha solution (Pir-HNTs) and (ii) the functionalization with phenylboronic acid (in particular with benzene-1,4-diboronic acid: the sample is denoted as HNT-BOA). Interestingly, both strategies enhance the performance of the multicomponent reaction. Pir-HNTs and HNT-BOA show an increased reactivity (72% and 89% yield, respectively) in comparison with pristine HNTs (52%). Additionally, Pir-HNTs can be reused up to five times without significant performance loss. Moreover, the method also displays good reaction scope, as demonstrated by the preparation of 12 different 3,4-dihydropyrimidinones in up to 71% yield. Therefore, the described strategies are promising for enhancing the acidity of the HNTs as catalysts for the organic reaction.

**Keywords:** halloysites nanotubes; solid acids; heterogeneous catalysts; multicomponent reactions; Biginelli reaction; 3,4-dihydropyrimidinones



**Citation:** Yu, J.; Mateos, J.; Carraro, M. Halloysite Nanotubes as Bimodal Lewis/Brønsted Acid Heterogeneous Catalysts for the Synthesis of Heterocyclic Compounds.

*Nanomaterials* **2023**, *13*, 394. <https://doi.org/10.3390/nano13030394>

Academic Editor: Alexey Pestryakov

Received: 28 December 2022

Revised: 13 January 2023

Accepted: 16 January 2023

Published: 18 January 2023



**Copyright:** © 2023 by the authors. Licensee MDPI, Basel, Switzerland. This article is an open access article distributed under the terms and conditions of the Creative Commons Attribution (CC BY) license (<https://creativecommons.org/licenses/by/4.0/>).

## 1. Introduction

Acid catalysts play a crucial role in the activation of organic molecules, thus significantly promoting various important organic reactions [1]. Although mineral acids (i.e., H<sub>2</sub>SO<sub>4</sub> and HCl) demonstrate high activity, they suffer from various shortcomings, such as reactor corrosion and poor catalyst separation and reuse. To this end, solid acidic catalysts have been designed to replace the mineral acids, with the multiple advantages of easier product separation and good catalysts recyclability [2–4]. However, the synthesis of an efficient solid acid with desirable catalytic performance, facile preparation, high environmental compatibility, as well as high thermal or chemical stability remains challenging [5].

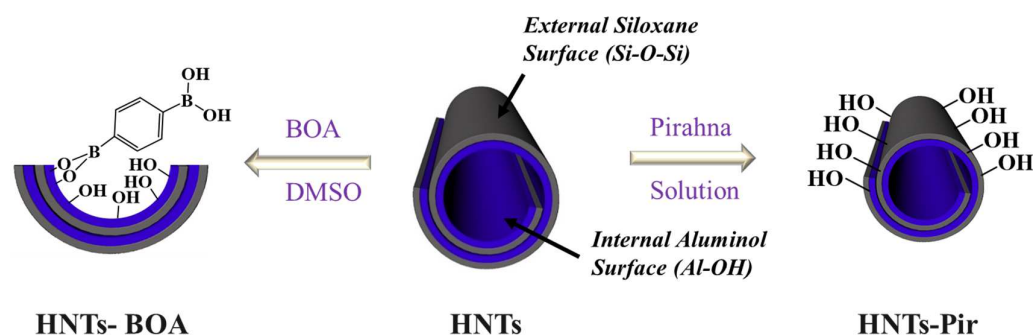
Halloysite is a naturally available, two-layered aluminosilicate similar to kaolin, whereby the packing disorder generated by the neighboring alumina and silica layers forces them to curve and roll up, thus forming stable multi-layered tubes [6]. Halloysite nanotubes (HNTs) have been widely utilized as scaffolds for supporting metal or metal oxide nanoparticles (NPs) due to their low-cost, reduced environmental toxicity, and surface hydroxyl groups available for functionalization [7–9]. Nowadays, a limited number of literature reports describe the use of HNTs as solid acidic catalysts [10]. The common strategies to enable their catalytic use are (i) the conversion of the hydroxyl moieties into

acidic groups or (ii) the treatment with an acidic solution. However, we think that extensive efforts are still needed to further enhance the performance of HNT-based acidic catalysts and extend their applications [11,12]. To the best of our knowledge, acidic HNT have only been applied to selective Prins cyclizations [13–15] and to the synthesis of naphthopyranopyrimidine derivatives through a three-component reaction between  $\beta$ -naphthol, aldehydes, and *N,N*-dimethylbarbituric acid [16,17].

Multicomponent reactions (MCRs) are reactions integrating more than two starting reagents into one single product. Due to the multiple advantages of atom economy, simplicity, convergence, and flexibility, MCRs are elegant alternatives for substituting multistep synthetic processes [18]. Moreover, such reactions provide a fascinating strategy to construct various heterocycles with meticulously designed features. MCRs include the Passerini, Ugi, Hantzsch, and Biginelli reactions, among many others [19]. Specifically, the Biginelli reaction has attracted enormous attention due to the essential therapeutic and pharmacological properties of its dihydropyrimidinone (DHPM) products [20]. DHPMs are not only medical synthons with excellent biological activities (e.g., for their antitumor, antibacterial, antiviral, and anti-inflammatory properties), but these types of compounds are also important natural products [21,22].

In general, acidic catalysts are required to improve the efficiency of the Biginelli reaction. Recently, some common Brønsted acids (such as  $H_2SO_4$  and  $HCl$ ) or Lewis acids (i.e.,  $LiClO_4$ ,  $BiCl_3$ ,  $FeCl_3$ ,  $LaCl_3$ ,  $Mn(OAc)_3$ ,  $Cu(OTf)_2$ ) [23,24] were employed as efficient catalysts for this transformation. However, all these inorganic acids and transition metal salts suffered from issues of being corrosive, toxic, and/or difficult to separate/reuse. Although some heterogeneous catalysts (i.e., metal–organic frameworks (MOFs) [25–28], covalent–organic frameworks (COFs) [29],  $CoFe_2O_4@SiO_2-NH_2-Co^{II}$  [30]) were also applied for this MCR, their syntheses usually require multistep processes and tedious procedures. Therefore, it is highly desirable to develop other facile strategies for the synthesis of heterogeneous acid catalysts for the Biginelli reaction.

Herein, we show two strategies for increasing the amount of acidic sites on the HNTs, aiming at improving the performance of HNTs for the Biginelli reaction. On the one hand, we treated HNTs with piranha solution to remove the impurities and activate the surface of HNTs by exposing more acidic sites on the outer silica layer [31]. The  $NH_3$ -temperature programmed desorption ( $NH_3$ -TPD) results indicated that the treatment with piranha solution increases the amount of Lewis acid sites on the HNTs. On the other hand, we grafted a boronic acid (BOA) on the inner lumen surface of HNTs to introduce additional acidic sites, since boronic acids are widely used and soluble in Lewis/Brønsted acid catalysts for organic reactions [32–34]. A diboronic acid was, thus, firmly immobilized, preferably on the internal wall of the HNTs (Scheme 1), exploiting one  $-B(OH)_2$  functionality for grafting the alumina while retaining the availability of the other for acidic catalysis. The resulting nano-hybrid can be easily separated from the reaction mixture for reuse.



**Scheme 1.** Modification of HNTs following two different approaches: (right) Pir-HNTs obtained by treatment with piranha solution, and (left) HNT-BOA obtained by grafting the diboronic acid inside the HNTs lumen.

The performances of obtained HNT-based acid catalysts prepared by the above-mentioned strategies were then demonstrated for the Biginelli reaction, showing that the HNTs with boronic acid displayed slightly higher activity than the HNTs treated with the piranha solution.

## 2. Materials and Methods

### 2.1. Reagents

Halloysite nanotubes (HNTs), anhydrous toluene, acetonitrile, ethanol, dichloromethane, dimethyl sulfoxide (DMSO), sulfuric acid (95–98 wt%), hydrogen peroxide (30 wt%), benzene-1,4-diboronic acid (BOA), ethyl acetoacetate, urea, thiourea, 3-chlorobenzaldehyde (97%), 4-chlorobenzaldehyde (97%), 2-chlorobenzaldehyde (99%), p-tolualdehyde (97%), and p-anisaldehyde (98%) were all purchased from Sigma-Aldrich.

### 2.2. Characterizations

NMR spectra were recorded on Bruker 400 Avance III HD equipped with a BBI-z grad probe head 5 mm.

High-Resolution Mass Spectra (HRMS) were collected using a Waters GCT gas chromatograph coupled with an electron ionization time-of-flight mass spectrometer (GC/MS-TOF).

FTIR spectra were obtained with solid samples on a Nicolet 5700 FT-IR instrument in ATR mode.

NH<sub>3</sub>-temperature programmed desorption (NH<sub>3</sub>-TPD) measurements were carried out on a TPDRO-1100-Omnistar with a thermal conductivity detector (TCD).

The in situ FTIR spectra during desorption of pyridine were measured on a Thermo Nicolet 380 FTIR spectrometer.

Thermogravimetric analyses (TGA) of samples were performed on a Q5000 IR instrument (TA Instruments) and collected in N<sub>2</sub> or air upon equilibration at 100 °C, with a subsequent temperature ramp (10 °C/min) up to 1000 °C.

### 2.3. Procedures

- Grafting of boronic acid inside the lumen of HNTs

200 mg pristine HNTs and 200 mg benzene-1,4-diboronic acid (BOA) were added to 20 mL of anhydrous dimethyl sulfoxide (DMSO) under a nitrogen atmosphere, and the resulting suspension was sonicated for 30 min. After sonication, the mixture was heated at 90 °C under reflux, for 24 h, under stirring. Then, the solid phase was separated by centrifugation and washed with ethyl acetate, methanol and dichloromethane, sequentially. In the end, the prepared HNTs were kept for 24 h under a vacuum for drying. The functionalized nanotubes were labeled as HNT-BOA and characterized by FTIR and TGA analyses [35].

- Activation treatment of HNTs

The activation procedure was already explained elsewhere [31]. The activated HNTs were denoted as Pir-HNTs and were additionally investigated by NH<sub>3</sub>-TPD.

- General procedure for the synthesis of 3,4-dihydropyrimidinones

The synthesis of the 3,4-dihydropyrimidinones followed a procedure described in literature with minor changes [18]. The reaction was performed in a 25 mL round bottom flask under an N<sub>2</sub> atmosphere. The substrates were added with a 1:1:1.5 stoichiometric ratio of ethyl acetoacetate (2 mmol), aldehyde (2 mmol), and urea (3 mmol) in 10 mL of acetonitrile. After the addition of 150 mg of HNTs, the mixture was kept under stirring under reflux for 38 h. After that, the catalysts were separated by filtration without waiting for the reaction mixture to cool down and washed with 20 mL of warm ethanol to remove the adsorbed reagents and products. The filtrated solution, together with 50 mL of washing ethanol, was transferred into crushed ice. As the ice melted, products appeared as white precipitates. Then, the products were purified by ethanol washing, dried under vacuum,

and weighed to calculate the isolated yield. All obtained products were characterized by  $^1\text{H}$  and  $^{13}\text{C}$  NMR and HRMS. Meantime, the separated catalysts were washed with water and ethanol, and dried in a desiccator, ready for the recycling tests.

### 3. Results and Discussion

#### 3.1. Synthesis of Halloysite Nanotube-Based Acid Catalysts

Firstly, we prepared two HNT-based acid catalysts, as shown in Scheme 1. HNTs functionalized with boronic acid on the internal wall (i.e., HNT-BOA) were synthesized by heating the mixture of HNTs and boronic acid at  $90^\circ\text{C}$  under reflux for 24 h in dimethyl sulfoxide (see experimental part). The piranha-etched HNTs (i.e., Pir-HNTs) were treated with piranha solution at  $90^\circ\text{C}$  for 1 h.

Figure 1a displays the FTIR spectra of samples, including pristine HNTs, Pir-HNTs (i.e., after treatment of piranha solution), and HNT-BOA (i.e., functionalized with boronic acid). In the case of HNTs, the peaks situated at  $3698\text{ cm}^{-1}$  and  $3621\text{ cm}^{-1}$  are ascribed to the stretching vibration of Al–OH at the inner surfaces and inner interfaces (interface between the Si–O tetrahedron and Al–O octahedron) of HNTs, respectively. The bands at  $940\text{ cm}^{-1}$  (very weak) and  $912\text{ cm}^{-1}$  result from the deformation of Al–OH at the inner surface and inner interface, respectively [36,37]. The peaks at  $1089\text{ cm}^{-1}$  and  $1031\text{ cm}^{-1}$  are assigned to the in-plane Si–O stretching, while the ones at  $1114\text{ cm}^{-1}$  and  $755\text{ cm}^{-1}$  are related to perpendicular Si–O stretching. The peak situated at  $790\text{ cm}^{-1}$  corresponds to the symmetric stretching of Si–O [36]. After the treatment with piranha solution, there are two additional broad signals located at  $3450\text{ cm}^{-1}$  and  $1210\text{ cm}^{-1}$ , corresponding to Si–OH vibration and Si–O–Si stretching vibration, respectively. This observation indicates that a higher amount of hydroxyl groups is present, while amorphous silica is also produced [38].

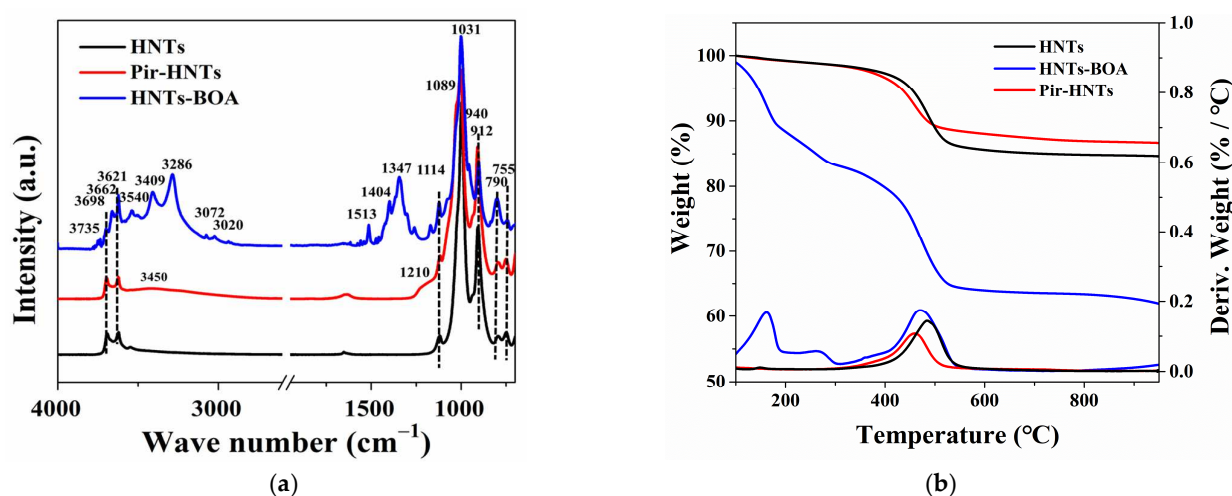


**Figure 1.** (a) FTIR absorbance spectra of commercial HNTs, activated HNT samples (i.e., Pir-HNTs), HNTs functionalized by boronic acid (i.e., HNT-BOA); (b) TGA curves of commercial HNTs, activated HNT samples (i.e., Pir-HNTs), HNTs functionalized by boronic acid (i.e., HNT-BOA).

The blue line in Figure 1 shows the spectrum of HNTs after grafting the benzene-1,4-diboronic acid (BOA). The intensity of the peak at  $3698\text{ cm}^{-1}$  is substantially reduced after the functionalization, due to the loss of the –OH groups upon reaction with the diboronic acid. Meanwhile, the band at  $3621\text{ cm}^{-1}$  retains its intensity, indicating that the hydroxyl groups located at the inner interfaces cannot react. The new peaks located at  $3409\text{ cm}^{-1}$  and  $3286\text{ cm}^{-1}$  correspond to the stretching vibration of the –OH groups linked to boron in the boronic acid [35]. The peak at  $1347\text{ cm}^{-1}$  can be attributed to B–O stretching, confirming the presence of boronic acid in the functionalized sample HNT-BOA [39,40]. Moreover, the absorption bands at  $3020\text{ cm}^{-1}$  and  $3072\text{ cm}^{-1}$  are due to the C–H stretching vibration of the phenyl ring, while  $1404\text{ cm}^{-1}$  and  $1513\text{ cm}^{-1}$  result from the benzene skeleton vibration. Notably, all the peaks corresponding to the Si–O–Si and Si–O stretching are well kept

in the spectrum of HNT-BOA, implying that the BOA is selectively grafted on the inner lumen surface of HNTs rather than the exterior surface. Besides all the bands for vibrations of halloysites and BOA, other characteristic peaks, corresponding to the small amount of solvent DMSO intercalation, can be observed: the weak peaks centered at  $3735\text{ cm}^{-1}$  and  $3662\text{ cm}^{-1}$  are related to hydrogen bonds generated between  $-\text{OH}$  at the inner lumen surface of HNTs and  $\text{S}=\text{O}$  groups of DMSO [41,42].

TGA measurements were used to characterize the samples and to determine the amount of BOA grafted on the HNTs (Figure 1b). The sample of HNTs after the treatment of piranha solution displays a lower overall mass loss of 12.2% than that without the treatment (15.1%) due to the removal of impurities and Al species during the treatment. As already reported, the small mass loss below  $300\text{ }^{\circ}\text{C}$  for HNTs is ascribed to the removal of adsorbed and interlayer water [37,43]. In the case of HNT-BOA, the weight loss in the temperature range of  $50\text{--}300\text{ }^{\circ}\text{C}$  is larger than that of HNTs without BOA, which may be due to the loss of intercalated DMSO and the adsorption of free BOA on the surfaces [44,45]. The mass loss in the range of  $300\text{--}550\text{ }^{\circ}\text{C}$  can be assigned to the dehydroxylation of the Al-OH and Si-OH sites of HNT in all three samples. Notably, the HNT-BOA sample displays a larger weight loss than that of HNTs without BOA; indeed, the additional weight loss can be attributed to the thermal decomposition of grafted BOA [46], calculated to be ca. 5.6 wt%.

To investigate the nature of the acidic sites on the HNTs and pir-HNTs, IR spectroscopy of adsorbed pyridine (Py-IR) measurements was performed on these two samples (Figure 2). Both samples demonstrated various peaks corresponding to pyridine adsorbed on the Lewis acid (LA) sites ( $1601$  and  $1448\text{ cm}^{-1}$ ) and Brønsted acid (BA) sites ( $1548\text{ cm}^{-1}$ ) [47,48]. Moreover, the type of acidic sites for the peak at  $1492\text{ cm}^{-1}$  cannot be distinguished by Py-IR, and such a peak is usually assigned to both LA and BA sites [40]. The amount of different kinds of acid sites was further quantified according to the peak area. As shown in Table S1, despite the nearly similar amount of BA sites on them, the amount of LA sites on the pir-HNTs is 1.84-fold higher than that of HNTs at  $40\text{ }^{\circ}\text{C}$ , suggesting that the treatment of piranha solution can significantly increase the number of LA sites on the HNTs but has little impact on that of BA sites. With the temperature increasing from  $40$  to  $200$  and  $350\text{ }^{\circ}\text{C}$ , the number of LA sites on both samples gradually decrease, due to the loss of weaker LA sites. Notably, at  $350\text{ }^{\circ}\text{C}$ , the number of LA sites on the pir-HNTs is still as high as  $22.79\text{ }\mu\text{mol/g}$  corresponding to strong LA sites (SLA), 3.74-fold to that of HNTs, indicating that the piranha solution can also markedly enhance the strength of LA sites for promoting the generation of SLA sites. Interestingly, the strength of BA is also enhanced through the treatment of piranha solution, and the amount of BA for the pir-HNTs ( $21.57\text{ }\mu\text{mol/g}$ ) is much higher than that of HNTs ( $9.00\text{ }\mu\text{mol/g}$ ) at  $350\text{ }^{\circ}\text{C}$ . The acidic sites on the above two samples were further examined via the method of  $\text{NH}_3$ -temperature programmed desorption ( $\text{NH}_3$ -TPD, Figure 2b). There are two desorption peaks centered at around  $150\text{ }^{\circ}\text{C}$  and  $700\text{ }^{\circ}\text{C}$  in both cases, which correspond to BA and SLA sites on the surface of HNTs, respectively [47]. After the treatment with piranha solution, the peak of weak acid sites moves from  $131\text{ }^{\circ}\text{C}$  for the HNTs, and to  $165\text{ }^{\circ}\text{C}$  for the Pir-HNTs, suggesting that the strength of BA sites is enhanced for Pir-HNTs. Moreover, compared with the HNTs, the intensity of the peak centered at  $673\text{ }^{\circ}\text{C}$  for the Pir-HNTs is increased, indicating that the piranha solution treatment can increase the number of strong acidic sites on the HNTs. However, the amount of super acidic sites ( $700\text{--}800\text{ }^{\circ}\text{C}$ ) decreased after piranha solution treatment. Nevertheless, according to the Sabatier principle, the super strong acidic sites may cause excessive adsorption of molecules, which may hinder the reactivity. Thus, the decreased amount of super-strong acidic sites after the treatment may be beneficial for the multicomponent reaction [49].

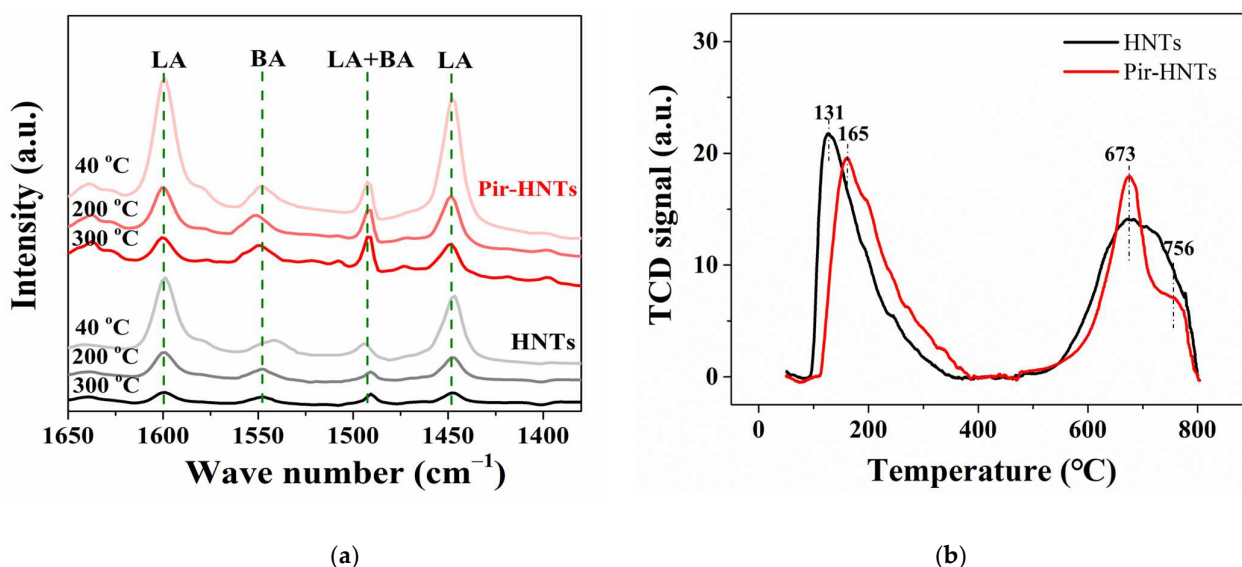


**Figure 2.** (a) Py-IR spectra of commercial HNT and activated HNT samples (i.e., Pir-HNTs) at different desorption temperatures: 40, 200, and 350 °C; (b) NH<sub>3</sub>-TPD profiles of commercial HNT and activated HNT samples (i.e., Pir-HNTs). TCD = thermal conductivity detector.

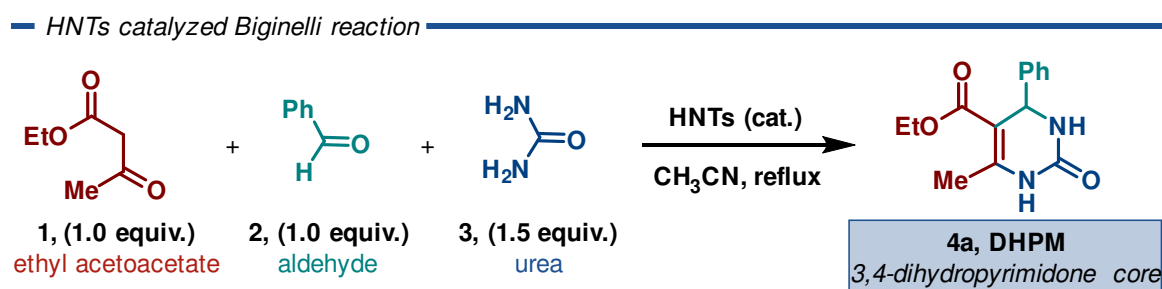
Therefore, the results of Py-IR match well with those of NH<sub>3</sub>-TPD and undoubtedly verify that the piranha solution treatment can markedly increase the amount of LA sites, especially SLA sites, and enhance the strength of BA sites on the HNTs.

It is reported that HNTs possess both Brønsted and Lewis acid sites. The Brønsted acid sites originated from the acidic OH-groups (H<sub>3</sub>O<sup>+</sup>), while Lewis acid sites are offered by the coordinatively unsaturated Al<sup>3+</sup> ions [15,50,51]. As described in the previous literature, we found that piranha treatment could remove the impurities, including Na<sup>+</sup>, K<sup>+</sup>, etc., from HNTs, slightly enlarge the lumen cavity and significantly increase the specific surface area [38]. As a result of the three effects induced by the piranha solution, the number of Al acidic sites and of Si-OH groups can both be increased.

NH<sub>3</sub>-TPD and Py-IR methods cannot be used to measure the acidic properties of HNT-BOA since the benzene-1,4-diboronic acid undergoes thermal decomposition, as shown in the above TGA results. Nevertheless, boronic acids are well-known acid catalysts (both Brønsted and Lewis acid) that have been used as catalysts for various organic reactions [34,52–54]. In the future, the acidity may be investigated by potentiometric acid titration (PT).

### 3.2. Catalytic Performance of HNTs in the Biginelli Reaction

The Biginelli reaction is a well-known acid-catalyzed process, and it has drawn extensive attention from chemists due to the attractive pharmacological properties of its DHPM products accessible through this manifold. The catalytic performance of pristine and modified HNTs was evaluated using the Biginelli reaction as a model reaction for generating 3,4-dihydropyrimidinones using widely available feedstock materials. The reaction was carried out under optimized conditions: a 1:1:1.5 stoichiometric ratio of ethyl acetoacetate **1** (2 mmol), aldehyde **2** (2 mmol), and urea **3** (3 mmol) in 10 mL of acetonitrile under reflux (Scheme 2).



**Scheme 2.** Biginelli reaction catalyzed by HNTs.

Figure 3 shows the isolated yield reaction profiles of the Biginelli reaction over time in the presence of different HNTs catalysts. The tested catalysts were: (i) commercial HNTs (black squares, Figure 3), (ii) Brønsted acid-activated HNT samples (Pir-HNTs, red triangles, Figure 3), and (iii) Lewis acid HNTs functionalized (HNT-BOA, blue circles, Figure 3).

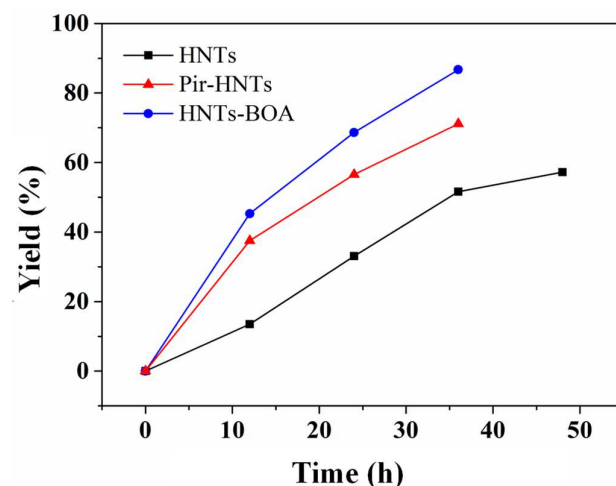


**Figure 3.** Yields of products dependent on the reaction time over different catalysts, including commercial HNTs, Brønsted-acid-activated HNTs (Pir-HNTs), and HNTs functionalized by boronic acid (HNT-BOA).

In order to carefully determine the reaction performance over time, the yields were calculated after product isolation and purification for all the catalysts. We started our investigations by testing the activity of HNTs. It is worth mentioning that pristine HNTs exhibited moderate activity in the Biginelli reaction due to the intrinsic presence of acidic sites on it. The yields of products catalyzed by HNTs gradually increased from 13% yield after 12 h to 52% yield after 36 h. Under a longer reaction time (48 h), the yield of **4a** (57%) is only slightly improved. Interestingly, both silica and alumina, taken as reference compounds, did not allow to obtain yields higher than 10%, highlighting the importance of the two-layered aluminosilicate material as a catalyst (Table S2). Then, we decided to test the performances of the treated HNTs. In fact, the yields of **4a**, when catalyzed by piranha solution-treated HNTs, are 38% in 12 h and 72% in 36 h (three times faster than pristine HNTs). The enhanced catalytic performance of the Pir-HNTs is attributed to the increased number of acidic sites resulting from the treatment with piranha solution. Analogously, the HNTs grafted with the BOA sample exhibit the best catalytic performance among these three catalysts. In the case of utilizing HNT-BOA as a catalyst, the yields of DHPMs are 45% in 12 h and up to 87% after 36 h (almost five times faster than pristine HNTs). This enhancement by using HNT-BOA as catalysts suggests that the functionalization of HNTs with the BOA can efficiently boost the performance as acidic catalysts in MCR. To sum up, the experimental results indicated that both protocols are efficient in increasing acidity sites, leading to a higher activity of related acid-catalyzed reactions.

One of the most reliable tests for the versatility of a heterogeneous catalyst is by checking its recyclability. For this reason, Pir-HNTs and HNT-BOA were evaluated, as shown in Figure 4. After every reaction, the catalyst was recovered by simply filtrating the reaction mixture and washing the obtained solid with ethanol and water. Clearly, the Pir-HNTs demonstrated excellent stability for the Biginelli reaction (red bars, Figure 4) with minor activity loss during five recycles (less than 10% yield erosion). In contrast, an activity decay of up to 25% was observed with the HNT-BOA (blue bar, Figure 4) after five recycles. These results suggest a poorer stability of the HNT-BOA in this system when overused.

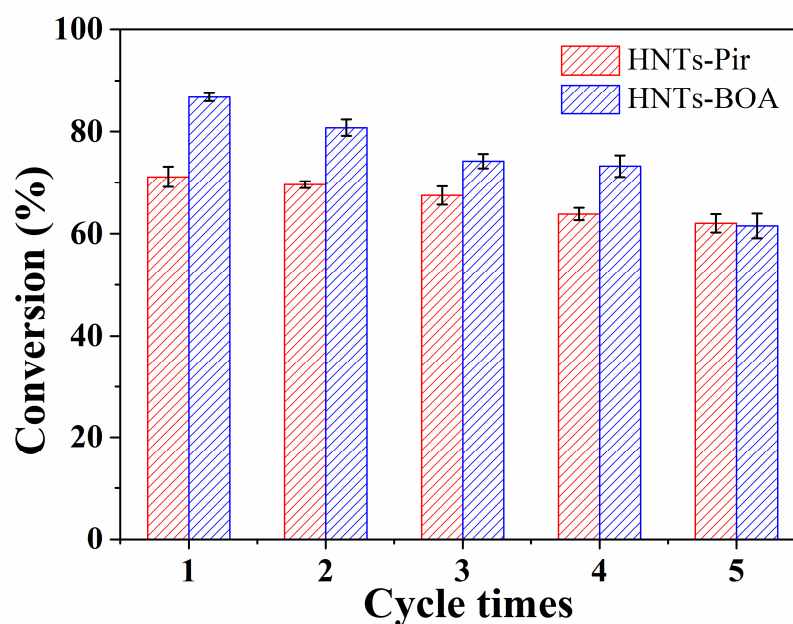


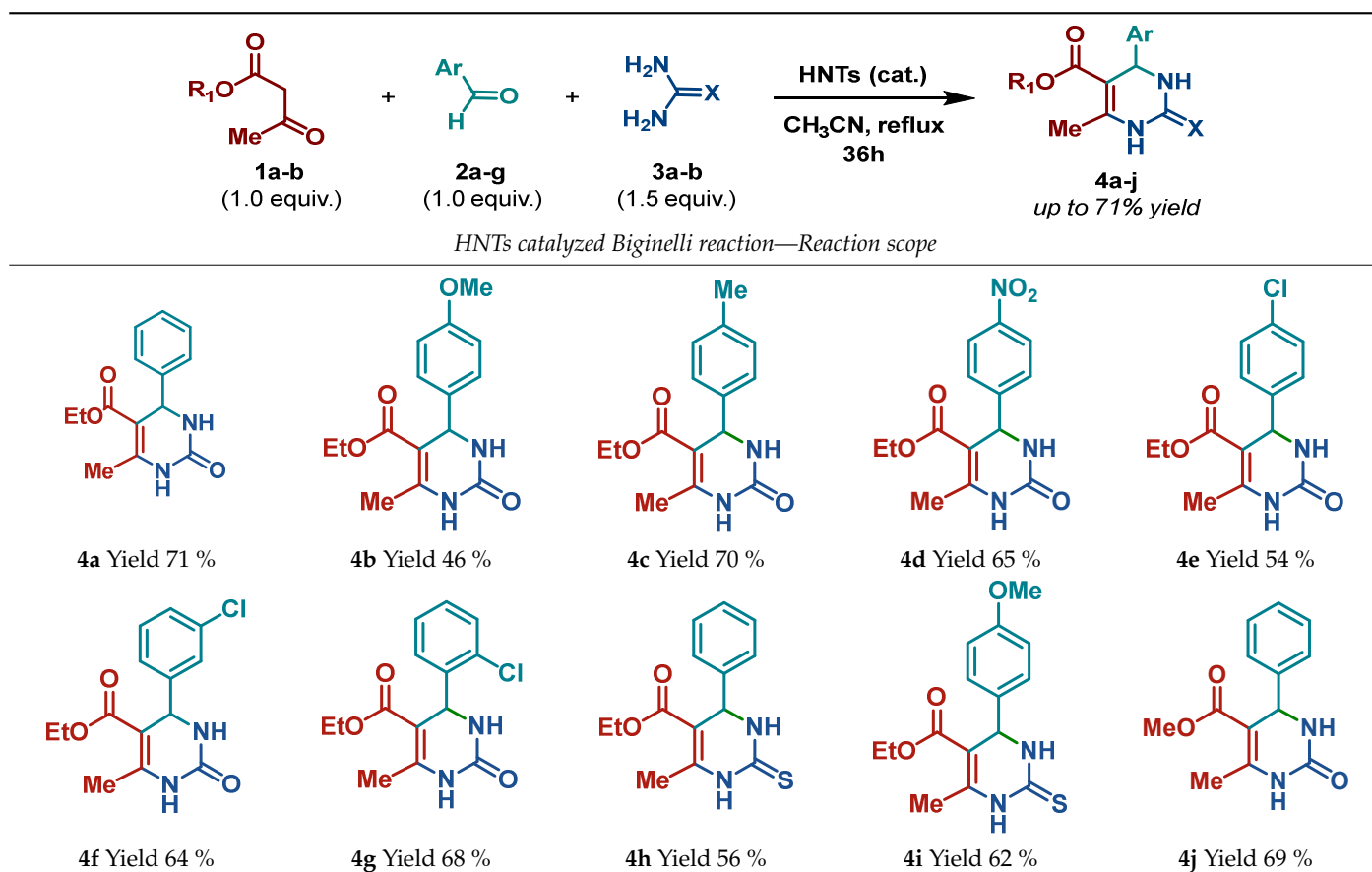
**Figure 4.** The recycling test of Pir-HNTs and HNT-BOA for Biginelli reaction to produce 3,4-dihydropyrimidinones (**4a**).

The reason for the decreased activity in subsequent recycles can be ascribed to the mechanical damages occurring during mixing and reaction workup. Moreover, HNT-BOA is more susceptible to the leaching of organic groups.

Given that the treatment with piranha solution is easier and amenable to scaling-up than the grafting of boronic acid and owing to their higher robustness during catalytic turnover, Pir-HNTs were selected to explore the scope of the HNTs catalyzed via Biginelli reaction (Table 1).

On the one side, diversely substituted aldehydes **2a–g** bearing either electron-donating or electron-withdrawing groups were tested. The functional group on the aryl moiety of the aldehydes had no significant effect on the formation of DHPM products **4a–h**. Electron-rich and electron-poor aldehydes achieved 3,4-dihydropyrimidinones in good yields (from 46 to 71% yield). At the same time, substituting the urea **3a** with thiourea **3b** furnished **4i** in a good 62% yield. Analogously, using methyl acetoacetate **1b**, also yielded **4j** in good yields (69%), altogether showing the high versatility of HNT catalysts for MCRs.

The activity of our catalysts toward the **4a** product has been compared with that of other solid acid catalysts, collecting relevant data in Table S3 [55–58]. The performance of HNTs derivatives is generally lower than that of other reported catalysts. Nevertheless, the synthetic procedure of our catalysts is easier and performed under milder conditions. Moreover, they are derived from naturally abundant HNTs with the advantages of being cheaper and environmentally friendly.

**Table 1.** Versatility of the HNTs catalyzed via Biginelli reaction.

Reaction Conditions: 1 (2.0 mmol), 2 (2.0 mmol), 3 (2.0 mmol), catalysts (150 mg), 10 mL CH<sub>3</sub>CN under reflux temperature, 36 h. Isolated yields after recrystallization are reported.

#### 4. Conclusions

In conclusion, we have demonstrated that HNTs can be employed as robust acid catalysts for the Biginelli reaction to produce heterocyclic compounds, enhancing the catalytic activity of pristine HNTs via two different treatment strategies. One approach is to expose more acidic sites of the HNTs by treatment with a piranha solution. The other strategy is to introduce additional acid sites into HNTs via the functionalization with phenylboronic acid. Both strategies were found to be efficient in increasing the performance of the Biginelli reaction. By comparing the two strategies, we found that the piranha treatment is more facile to be operated, and the catalyst displayed good recycling ability. Additionally, the HNTs functionalized with boronic acid showed even higher yields compared to the Pir-HNTs. Meanwhile, as a grafted catalyst, the HNT-BOA may also have the problem of releasing BOA during the recycling of the reaction due to the cleavage of B–O bonds. Nevertheless, since boronic acid can be considered a generally acid catalyst, the HNT-BOA may have the potential to apply for some specific reactions which may not occur with Pir-HNTs. In addition, the HNT-BOA catalyst can be regarded as a micro-reactor operating inside the lumen cavity of the HNTs, which may facilitate the reaction due to spatial confinement effects.

Overall, both strategies are efficient in enhancing the acidity of the HNTs for organic reaction and offer further possibilities according to the different requirements. Although other synthetic heterogeneous systems appear faster than the present solid acid (with conversions occurring in 0.5–2 h), we believe that the activated HNTs should deserve more attention, being cheaper and easier to prepare [17–21].

**Supplementary Materials:** The following supporting information can be downloaded at: <https://www.mdpi.com/article/10.3390/nano13030394/s1>, Figures S1–S20: NMR spectra; Table S1: The amount different kinds of acid sites on the HNTs and pir-HNTs determined by the measurement of Py-IR; Table S2: Yields of product **4a** over different catalysts; Table S3: Comparison of HNTs activity with respect to other reported catalysts toward Biginelli reaction.

**Author Contributions:** Conceptualization and methodology by J.Y., J.M.; investigation and original draft preparation by J.Y.; supervision, writing—review and editing, M.C. All authors have read and agreed to the published version of the manuscript.

**Funding:** This research was funded by the Department of Chemical Sciences of Padova University, grant number: P-DiSc#11NExuS\_BIRD2019-UNIPD.

**Data Availability Statement:** Additional information is available from the authors.

**Acknowledgments:** J.Y. acknowledges support from the Chinese Scholarship Council for funding her PhD in Science and Engineering of Materials and Nanostructures at the University of Padova. We thank Luca Dell’Amico for the helpful discussions.

**Conflicts of Interest:** The authors declare no conflict of interest. The funders had no role in the design of the study, in the collection, analyses, or interpretation of data, in the writing of the manuscript, or in the decision to publish the results.

## References

1. Busca, G. Acid catalysts in industrial hydrocarbon chemistry. *Chem. Rev.* **2007**, *107*, 5366–5410. [[CrossRef](#)] [[PubMed](#)]
2. Corma, A. Solid acid catalysts. *Curr. Opin. Solid State Mater. Sci.* **1997**, *2*, 63–75. [[CrossRef](#)]
3. Huang, Y.B.; Fu, Y. Hydrolysis of cellulose to glucose by solid acid catalysts. *Green Chem.* **2013**, *15*, 1095–1111. [[CrossRef](#)]
4. Sartori, G.; Maggi, R. Use of Solid Catalysts in Friedel-Crafts Acylation Reactions. *Chem. Rev.* **2006**, *106*, 1077–1104. [[CrossRef](#)]
5. Clark, J.H. Solid acids for green chemistry. *Acc. Chem. Res.* **2002**, *35*, 791–797. [[CrossRef](#)]
6. Yuan, P.; Tan, D.; Annabi-Bergaya, F. Properties and applications of halloysite nanotubes: Recent research advances and future prospects. *Appl. Clay Sci.* **2015**, *112*, 75–93. [[CrossRef](#)]
7. Massaro, M.; Colletti, C.; Lazzara, G.; Milioto, S.; Noto, R.; Riela, S. Halloysite nanotubes as support for metal-based catalysts. *J. Mater. Chem. A* **2017**, *5*, 13276–13293. [[CrossRef](#)]
8. Das, T.K.; Ganguly, S.; Bhawal, P.; Remanan, S.; Mondal, S.; Das, N.C. Mussel inspired green synthesis of silver nanoparticles-decorated halloysite nanotube using dopamine: Characterization and evaluation of its catalytic activity. *Appl. Nanosci.* **2018**, *8*, 173–186. [[CrossRef](#)]
9. Ghosh, S.K.; Das, T.K.; Ghosh, S.; Ganguly, S.; Nath, K.; Das, N.C. Physico-mechanical, rheological and gas barrier properties of organoclay and inorganic phyllosilicate reinforced thermoplastic films. *J. Appl. Polym.* **2020**, *138*, 49735. [[CrossRef](#)]
10. Abbasov, V.; Mammadova, T.; Aliyeva, N.; Abbasov, M.; Movsumov, N.; Joshi, A.; Lvov, Y.; Abdullayev, E. Catalytic cracking of vegetable oils and vacuum gasoil with commercial high alumina zeolite and halloysite nanotubes for biofuel production. *Fuel* **2016**, *181*, 55–63. [[CrossRef](#)]
11. Silva, S.M.; Peixoto, A.F.; Freire, C. HSO<sub>3</sub>-functionalized halloysite nanotubes: New acid catalysts for esterification of free fatty acid mixture as hybrid feedstock model for biodiesel production. *Appl. Catal. A Gen.* **2018**, *568*, 221–230. [[CrossRef](#)]
12. Mahajan, A.; Gupta, P. Halloysite nanotubes based heterogeneous solid acid catalysts. *New J. Chem.* **2020**, *44*, 12897–12908. [[CrossRef](#)]
13. Sidorenko, A.Y.; Kravtsova, A.; Il’ina, I.; Wärnå, J.; Korchagina, D.; Gatilov, Y.V.; Volcho, K.; Salakhutdinov, N.; Murzin, D.Y.; Agabekov, V. Clay nanotubes catalyzed solvent-free synthesis of octahydro-2H-chromenols with pharmaceutical potential from (-)-isopulegol and ketones. *J. Catal.* **2019**, *380*, 145–152. [[CrossRef](#)]
14. Li-Zhulanov, N.; Mäki-Arvela, P.; Laluc, M.; Peixoto, A.F.; Kholkina, E.; Sandberg, T.; Aho, A.; Volcho, K.; Salakhutdinov, N.; Freire, C.; et al. Prins cyclization of (-)-isopulegol with benzaldehyde for production of chromenols over organosulfonic clays. *Mol. Catal.* **2019**, *478*, 110569. [[CrossRef](#)]
15. Sidorenko, A.Y.; Kravtsova, A.V.; Aho, A.; Heinmaa, I.; Volcho, K.P.; Salakhutdinov, N.F.; Agabekov, V.E.; Murzin, D.Y. Acid-modified Halloysite Nanotubes as a Stereoselective Catalyst for Synthesis of 2H-Chromene Derivatives by the Reaction of Isopulegol with Aldehydes. *ChemCatChem* **2018**, *10*, 3950–3954. [[CrossRef](#)]
16. Kumar, P.; Gupta, P.; Sharma, C. Surface modified novel magnetically tuned halloysite functionalized sulfonic acid: Synthesis, characterization and catalytic activity. *Catal. Sci. Technol.* **2021**, *11*, 3775–3786. [[CrossRef](#)]
17. Samadani, M.; Asadi, B.; Mohammadpoor-Baltork, I.; Mirkhani, V.; Tangestaninejad, S.; Moghadam, M. Triazine bis(pyridinium) hydrogen sulfate ionic liquid immobilized on functionalized halloysite nanotubes as an efficient catalyst for one-pot synthesis of naphthopyranopyrimidines. *RSC Adv.* **2021**, *11*, 11976–11983. [[CrossRef](#)]
18. Dömling, A.; Wang, W.; Wang, K. Chemistry and Biology Of Multicomponent Reactions. *Chem. Rev.* **2012**, *112*, 3083–3135. [[CrossRef](#)]

19. Singh, M.S.; Chowdhury, S. Recent developments in solvent-free multicomponent reactions: A perfect synergy for eco-compatible organic synthesis. *RSC Adv.* **2012**, *2*, 4547–4592. [[CrossRef](#)]
20. Nagarajaiah, H.; Mukhopadhyay, A.; Moorthy, J.N. Biginelli reaction: An overview. *Tetrahedron Lett.* **2016**, *57*, 5135–5149. [[CrossRef](#)]
21. Debache, A.; Boumoud, B.; Amimour, M.; Belfaitah, A.; Rhouati, S.; Carboni, B. Phenylboronic acid as a mild and efficient catalyst for Biginelli reaction. *Tetrahedron Lett.* **2006**, *47*, 5697–5699. [[CrossRef](#)]
22. Huang, Y.; Yang, F.; Zhu, C. Highly Enantioselective Biginelli Reaction Using a New Chiral Ytterbium Catalyst: Asymmetric Synthesis of Dihydropyrimidines. *J. Am. Chem. Soc.* **2005**, *127*, 16386–16387. [[CrossRef](#)] [[PubMed](#)]
23. Sweet, F.; Fissekis, J.D. Synthesis of 3,4-dihydro-2(1H)-pyrimidinones and the mechanism of the Biginelli reaction. *J. Am. Chem. Soc.* **1973**, *95*, 8741–8749. [[CrossRef](#)]
24. Paraskar, A.; Dewkar, G.; Sudalai, A. Cu(OTf)<sub>2</sub>: A reusable catalyst for high-yield synthesis of 3,4-dihydropyrimidin-2(1H)-ones. *Tetrahedron Lett.* **2003**, *44*, 3305–3308. [[CrossRef](#)]
25. Krishna, B.; Payra, S.; Roy, S. Synthesis of dihydropyrimidinones via multicomponent reaction route over acid functionalized Metal–Organic framework catalysts. *J. Colloid Interface Sci.* **2022**, *607*, 729–741. [[CrossRef](#)]
26. Zhao, S.-Y.; Chen, Z.-Y.; Wei, N.; Liu, L.; Han, Z.-B. Highly Efficient Cooperative Catalysis of Single-Site Lewis Acid and Brønsted Acid in a Metal–Organic Framework for the Biginelli Reaction. *Inorg. Chem.* **2019**, *58*, 7657–7661. [[CrossRef](#)]
27. Pal, T.K.; De, D.; Senthilkumar, S.; Neogi, S.; Bharadwaj, P.K. A Partially Fluorinated, Water-Stable Cu(II)–MOF Derived via Transmetalation: Significant Gas Adsorption with High CO<sub>2</sub> Selectivity and Catalysis of Biginelli Reactions. *Inorg. Chem.* **2016**, *55*, 7835–7842. [[CrossRef](#)]
28. Verma, A.; De, D.; Tomar, K.; Bharadwaj, P.K. An Amine Functionalized Metal–Organic Framework as an Effective Catalyst for Conversion of CO<sub>2</sub> and Biginelli Reactions. *Inorg. Chem.* **2017**, *56*, 9765–9771. [[CrossRef](#)]
29. Yao, B.-J.; Wu, W.-X.; Ding, L.-G.; Dong, Y.-B. Sulfonic Acid and Ionic Liquid Functionalized Covalent Organic Framework for Efficient Catalysis of the Biginelli Reaction. *J. Org. Chem.* **2021**, *86*, 3024–3032. [[CrossRef](#)]
30. Allahresani, A.; Sangani, M.M.; Nasser, M.A.; Hemmat, K. CoFe<sub>2</sub>O<sub>4</sub>@SiO<sub>2</sub>-NH<sub>2</sub>-CoII NPs: An effective magnetically recoverable catalyst for Biginelli reaction. *Inorg. Chem. Commun.* **2020**, *118*, 107988. [[CrossRef](#)]
31. Yu, J.; Niedenthal, W.; Smarsly, B.M.; Natile, M.M.; Huang, Y.; Carraro, M. Au nanoparticles supported on piranha etched halloysite nanotubes for highly efficient heterogeneous catalysis. *Appl. Surf. Sci.* **2021**, *546*, 149100. [[CrossRef](#)]
32. Zheng, H.; McDonald, R.; Hall, D.G. Boronic Acid Catalysis for Mild and Selective [3+2] Dipolar Cycloadditions to Unsaturated Carboxylic Acids. *Chem. A Eur. J.* **2010**, *16*, 5454–5460. [[CrossRef](#)]
33. Sakakura, A.; Ohkubo, T.; Yamashita, R.; Akakura, M.; Ishihara, K. Brønsted Base-Assisted Boronic Acid Catalysis for the Dehydrative Intramolecular Condensation of Dicarboxylic Acids. *Org. Lett.* **2011**, *13*, 892–895. [[CrossRef](#)]
34. Hall, D.G. Boronic acid catalysis. *Chem. Soc. Rev.* **2019**, *48*, 3475–3496. [[CrossRef](#)]
35. Liu, F.; Bai, L.; Zhang, H.; Song, H.; Hu, L.; Wu, Y.; Ba, X. Smart H<sub>2</sub>O<sub>2</sub>-Responsive Drug Delivery System Made by Halloysite Nanotubes and Carbohydrate Polymers. *ACS Appl. Mater. Interfaces* **2017**, *9*, 31626–31633. [[CrossRef](#)]
36. Yuan, P.; Southon, P.D.; Liu, Z.; Green, M.E.; Hook, J.M.; Antill, S.J.; Kepert, C.J. Functionalization of Halloysite Clay Nanotubes by Grafting with  $\gamma$ -Aminopropyltriethoxysilane. *J. Phys. Chem. C* **2008**, *112*, 15742–15751. [[CrossRef](#)]
37. Yu, J.; Boudjelida, S.; Galiano, F.; Figoli, A.; Bonchio, M.; Carraro, M. Porous Polymeric Membranes Doped with Halloysite Nanotubes and Oxygenic Polyoxometalates. *Adv. Mater. Interfaces* **2022**, *9*, 2102152. [[CrossRef](#)]
38. Sun, P.; Liu, G.; Lv, D.; Dong, X.; Wu, J.; Wang, D. Effective activation of halloysite nanotubes by piranha solution for amine modification via silane coupling chemistry. *RSC Adv.* **2015**, *5*, 52916–52925. [[CrossRef](#)]
39. Nishiyabu, R.; Teraoka, S.; Matsushima, Y.; Kubo, Y. Fabrication of Soft Submicrospheres by Sequential Boronate Esterification and Their Dynamic Behavior. *ChemPlusChem* **2012**, *77*, 201–209. [[CrossRef](#)]
40. Matsushima, Y.; Nishiyabu, R.; Takanashi, N.; Haruta, M.; Kimura, H.; Kubo, Y. Boronate self-assemblies with embedded Au nanoparticles: Preparation, characterization and their catalytic activities for the reduction of nitroaromatic compounds. *J. Mater. Chem.* **2012**, *22*, 24124–24131. [[CrossRef](#)]
41. Breen, C.; D’Mello, N.; Yarwood, J. The thermal stability of mixed phenylphosphonic acid/water intercalates of kaolin and halloysite. A TG–EGA and VT-DRIFTS study. *J. Mater. Chem.* **2002**, *12*, 273–278. [[CrossRef](#)]
42. Mahrez, N.; Bendenia, S.; Marouf-Khelifa, K.; Batonneau-Gener, I.; Khelifa, A. Improving of the adsorption capacity of halloysite nanotubes intercalated with dimethyl sulfoxide. *Compos. Interfaces* **2015**, *22*, 403–417. [[CrossRef](#)]
43. Joussein, E.; Petit, S.; Fialips, C.-I.; Vieillard, P.; Righi, D. Differences in the dehydration-rehydration behavior of halloysites: New evidence and interpretations. *Clays Clay Miner.* **2006**, *54*, 473–484. [[CrossRef](#)]
44. Li, Y.; Zhang, Y.; Zhang, Y.; Sun, J.; Wang, Z. Thermal behavior analysis of halloysite–dimethylsulfoxide intercalation complex. *J. Therm. Anal. Calorim.* **2017**, *129*, 985–990. [[CrossRef](#)]
45. Cromwell, B.; Levenson, A.; Levine, M. Thermogravimetric analysis of aromatic boronic acids for potential flame retardant applications. *Thermochim. Acta* **2019**, *683*, 178476. [[CrossRef](#)]
46. Liu, X.; He, S.; Song, G.; Jia, H.; Shi, Z.; Liu, S.; Zhang, L.; Lin, J.; Nazarenko, S. Proton conductivity improvement of sulfonated poly(ether ether ketone) nanocomposite membranes with sulfonated halloysite nanotubes prepared via dopamine-initiated atom transfer radical polymerization. *J. Membr. Sci.* **2016**, *504*, 206–219. [[CrossRef](#)]

47. Zhao, Z.; Ran, J.; Jiao, Y.; Li, W.; Miao, B. Modified natural halloysite nanotube solely employed as an efficient and low-cost solid acid catalyst for alpha-arylstyrenes production via direct alkenylation. *Appl. Catal. A Gen.* **2016**, *513*, 1–8. [[CrossRef](#)]
48. Zhang, J.; Shi, K.; An, Z.; Zhu, Y.; Shu, X.; Song, H.; Xiang, X.; He, J. Acid–Base Promoted Dehydrogenation Coupling of Ethanol on Supported Ag Particles. *Ind. Eng. Chem. Res.* **2020**, *59*, 3342–3350. [[CrossRef](#)]
49. Che, M. Nobel Prize in chemistry 1912 to Sabatier: Organic chemistry or catalysis? *Catal. Today* **2013**, *218–219*, 162–171. [[CrossRef](#)]
50. Bergaya, F.; Lagaly, G. Chapter 1 General Introduction: Clays, Clay Minerals, and Clay Science. *Dev. Clay Sci.* **2006**, *1*, 1–18. [[CrossRef](#)]
51. Sidorenko, A.Y.; Kravtsova, A.; Wärnå, J.; Aho, A.; Heinmaa, I.; Il'ina, I.; Ardashov, O.; Volcho, K.; Salakhutdinov, N.; Murzin, D.Y.; et al. Preparation of octahydro-2H-chromen-4-ol with analgesic activity from isopulegol and thiophene-2-carbaldehyde in the presence of acid-modified clays. *Mol. Catal.* **2018**, *453*, 139–148. [[CrossRef](#)]
52. Sidera, M.; Fletcher, S. Rhodium-catalysed asymmetric allylic arylation of racemic halides with arylboronic acids. *Nat. Chem.* **2015**, *7*, 935–939. [[CrossRef](#)]
53. Zheng, H.; Ghanbari, S.; Nakamura, S.; Hall, D.G. Boronic Acid Catalysis as a Mild and Versatile Strategy for Direct Carbo- and Heterocyclizations of Free Allylic Alcohols. *Angew. Chem. Int. Ed.* **2012**, *51*, 6187–6190. [[CrossRef](#)]
54. Letsinge, R.L.; Dandegaonker, S.; Vullo, W.S.; Morrison, J. Organoboron Compounds. XIV.<sup>1,2</sup> Polyfunctional Catalysis by 8-Quinolineboronic Acid. *J. Am. Chem. Soc.* **1963**, *85*, 2223–2227. [[CrossRef](#)]
55. Zhang, H.; Hu, Q.; Liu, J.; Zhang, P.; Fu, S.; Wu, S. Iron–Organic Framework Nanoparticle-Supported Tungstosilicic Acid as a Catalyst for the Biginelli Reaction. *ACS Appl. Nano Mater.* **2022**, *5*, 16987–16995. [[CrossRef](#)]
56. Quan, Z.J.; Da, Y.X.; Zhang, Z.; Wang, X.C. PS–PEG–SO<sub>3</sub>H as an efficient catalyst for 3, 4-dihydropyrimidones via Biginelli reaction. *Catal. Commun.* **2019**, *10*, 1146–1148. [[CrossRef](#)]
57. Konkala, K.; Sabbavarapu, N.M.; Katla, R.; Durga, N.Y.V.; Reddy, V.K.; Prabhavathi Devi, B.L.A.; Prasad, R.B.N. Revisit to the Biginelli reaction: A novel and recyclable bioglycerol-based sulfonic acid functionalized carbon catalyst for one-pot synthesis of substituted 3, 4-dihydropyrimidin-2-(1H)-ones. *Tetrahedron Lett.* **2012**, *53*, 1968–1973. [[CrossRef](#)]
58. Yao, N.; Lu, M.; Liu, X.B.; Tan, J.; Hu, Y.L. Copper-doped mesoporous silica supported dual acidic ionic liquid as an efficient and cooperative reusability catalyst for Biginelli reaction. *J. Mol. Liq.* **2018**, *262*, 328–335. [[CrossRef](#)]

**Disclaimer/Publisher's Note:** The statements, opinions and data contained in all publications are solely those of the individual author(s) and contributor(s) and not of MDPI and/or the editor(s). MDPI and/or the editor(s) disclaim responsibility for any injury to people or property resulting from any ideas, methods, instructions or products referred to in the content.